J Mater Sci (2011) 46:1494–1501
DOI 10.1007/s10853-010-4951-0

Preparation of carbon spheres by low-temperature pyrolysis of cyclic hydrocarbons

N. Koprinarov · M. Konstantinova

Received: 3 June 2010 / Accepted: 24 September 2010 / Published online: 2 November 2010
© Springer Science+Business Media, LLC 2010

Abstract Low-temperature pyrolytic decomposition of xylene, benzene, toluene, and naphthalene was investigated as a low-cost method for synthesis of a large quantity of perfectly shaped pure carbon spheres. The reaction occurred in a closed iron container at temperatures in the range of 500–700 °C and under pressure of 20 MPa. Some of the experiments were carried out in the presence of distilled water in vapor state near to its critical point, under which conditions it reacted as a very strong oxidant. Transmission electron microscopy (TEM), scanning electron microscopy (SEM), energy-dispersive spectroscopy (EDS), and X-ray diffraction (XRD) analysis were used to investigate the properties of the material obtained. The results demonstrated that synthesis had proceeded in the following sequence: vaporization of hydrocarbon, hydrocarbon transformation to condensing drops of heavy hydrocarbons, then drop growth accompanied by continuous alteration of the heavy carbon compounds until their final carbonization. Synthesis in a closed space stimulated particle growth, and particle diameters reached 1 to 12 μm. Continuous condensation of vapor onto the resulting drops caused agglomeration of some of the spheres to form pearl-necklace-like chains when the spheres docked to one another in the course of growth. Carbon atoms in the spheres were arranged in concentric, incompletely closed graphitic shells, which made them stable up to 600 °C in air. Above this temperature, rapid sphere degeneration occurred. Oxygen reacted with carbon atoms situated at the shell edges during heating in air, with some remaining in the spheres; oxygen penetration increased with treatment temperature.

N. Koprinarov (✉) · M. Konstantinova
Central Laboratory of Solar Energy and New Energy Sources, Bulgarian Academy of Sciences, 72, Tzarigradsko Chaussee Blvd, 1784 Sofia, Bulgaria
e-mail: koprin@phys.bas.bg

Introduction

Following the discovery of carbon onions [1], fullerenes [2], and carbon nanotubes [3], the types of new carbon particle obtained as a result of intensive study of scientists worldwide now include carbon spheres. Despite a certain similarity with C_{60} and carbon onions, they are classified as a distinct group because of their relatively large size and properties similar to those of graphite. Interest in them results from their uniformity, chemical purity, high thermal stability, high chemical inertness, high packing density, and excellent conductivity. The availability of relatively easy realization and efficient synthesis methods for their preparation enables their application as adsorbents [4], catalysts [5, 6], anodes in lithium-ion batteries [7], electrodes in supercondensors [8], lubricants, and polymer and rubber additives. Most methods for their preparation use a pyrolytic process, with or without catalyst. The properties of the synthesized spheres and the degree of their graphitization depend on the temperature at which pyrolysis proceeds. Assuming the temperature range of 800–900 °C as a border between low and high temperature, spheres have been obtained from styrene, toluene, benzene, hexane, cyclohexane, and ethane [9], corn starch [10], commercial kerosene [11], poly(phenylcarbyne) [12], and carbon-based networks $[CR]_n$ (R = Ph, Me, H) [13] at relatively high temperature, and at lower temperatures they have been obtained from benzene, aniline, and nitrobenzene [14] and glucose (using the hydrothermal method) [8]. There also exist other methods for carbon sphere preparation, for instance through reaction of ferrocene and ammonium

carbonate in a sealed quartz tube [15], catalytic chemical vapor deposition [16] or arc discharge [17], but these are less relevant to the processes and results presented herein.

Experimental

Cyclic hydrocarbon decomposition experiments were carried out in a closed iron container hermetically sealed by a copper tightening. The tightening was pressed against the container outlet with the same pressure (20 MPa) for all experiments. Container temperature was measured directly at its surface. Container heating was done in a furnace. After the container was put in the furnace, its temperature started to rise at a rate of 20 °C/min. When the planned temperature was reached (in most cases, 600 °C) the container was cooled at a rate of 30 °C/min. More details of the experimental procedure have been described previously [18].

The materials investigated in this work were toluene, benzene, xylene, and naphthalene (purity 99.99%; Institute of Pure Compounds, Sofia University, Bulgaria). These materials were selected for their ability to create carbon spheres during our previous examinations of pyrolytic decomposition of ferrocene [18]. In those experiments the hydrocarbons served as carbon source. The starting material was placed in air. The quantity used depended on the volume of the container, which was fully filled. In some of the experiments, distilled water was added to the hydrocarbons at 1:3 water/hydrocarbon ratio. In the course of hydrocarbon decomposition, water played the role of oxidizer and, at the same time, decreased the space in which pyrolysis and carbon atom restructuring could proceed.

The chemical compositions, crystal structures, bonding, and thermal stability of the spheres produced in the experiments were characterized by transmission electron microscopy (TEM), scanning electron microscopy (SEM), energy-dispersive spectroscopy (EDS), X-ray diffraction (XRD), and infrared (IR) spectrometric standard investigations with no additional material treatment. That made the obtained results authentic.

Results and discussion

Some of the most significant peculiarities of the experiments described below are: (1) pyrolytic decomposition of the starting material and construction of the resulting structures proceed in the same space; (2) both of these processes occur simultaneously; and (3) the rate of the processes remains slow because of the relatively low temperature. Thus, this synthesis approach yields better understanding of the resulting formation, growth, and graphitization of the spheres obtained.

The starting materials were used in the liquid phase. After their evaporation temperature is reached, they vaporize, increasing the pressure in the container. Material decomposition starts above about 600 °C. Therefore, we consider this temperature of 600 °C as the minimum pyrolysis temperature. Questions relating to the different ways in which starting materials can be transformed into carbon nanostructures are in no way new; they have been considered in connection with similar methods for synthesis of a number of other types of nanoparticle from hydrocarbons [19, 20]. According to these references, during pyrolysis, simultaneous destruction of starting substances and gradual creation of increasingly complicated hydrocarbons occur until the graphite lattice is finally built. This is a temperature-dependent process. The low temperature used prevents simultaneous vapor decomposition and synthesis of sophisticated molecules in large molecular complexes (for instance, molecules collected in drop form). The evolution of all the molecules is not the same, as temperature gradients exist in the container, arising due to heat transfer from the container walls to its interior, further complicated by vapor formation and by the fact that the container temperature is constantly increasing due to the external heating.

Analysis of SEM images shows that, as a result of the factors mentioned above, the process of sphere formation is continuous and takes place in the presence of molecular complexes, the molecules of which are at different stages of transformation. Differences in their chemical composition, physical properties, and viscosity, in particular, are clearly noticeable when examining those deposited on the container cover. On the surface formed by the cover as well as the container walls, the same processes of formation and growth occur as in the volume, but proceeding on a solid surface, resulting in precipitation of a planar deposit. After synthesis is finished, zones can be noticed on the cover, supporting the presence of various hydrocarbon phases with different viscosities, as has long been presumed. Figure 1 shows a part of the layer deposited on the container cover (the photos in Figs. 1, 2, and 3 are turned by 180° to correspond to the layer's natural position on the lower surface of the cover). The layer has not been pulled off, and thus it is possible to assess its uniformity and morphology. As it has been broken in a natural way, the even edges indicate a homogeneous structure. The base layer (up to 1 μm thick) has more defects than the surface, indicating layer growth unevenness in the initial formation period. It can be concluded from Fig. 2 that this deposited material has existed in the form of a liquid with high viscosity for a certain period of time, since a drop has started to form. Then it graphitized and broke as the experiment finished. The continuously increasing viscosity of the pyrolytically obtained mass is why drop formation stops at

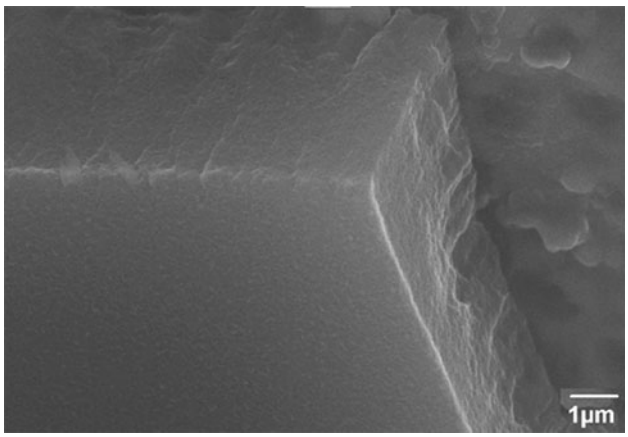

Fig. 1 A carbon deposit on the container cover

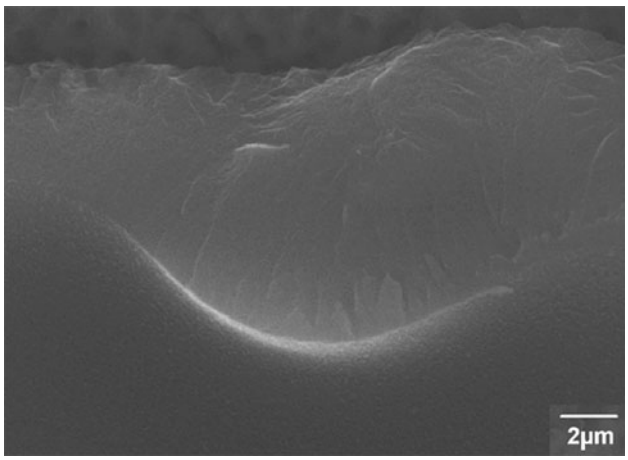

Fig. 2 A drop grown on the container cover

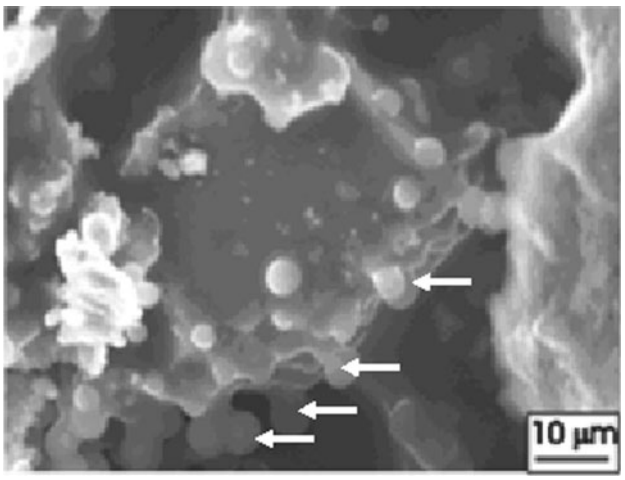

Fig. 3 Graphitized drops on the container cover

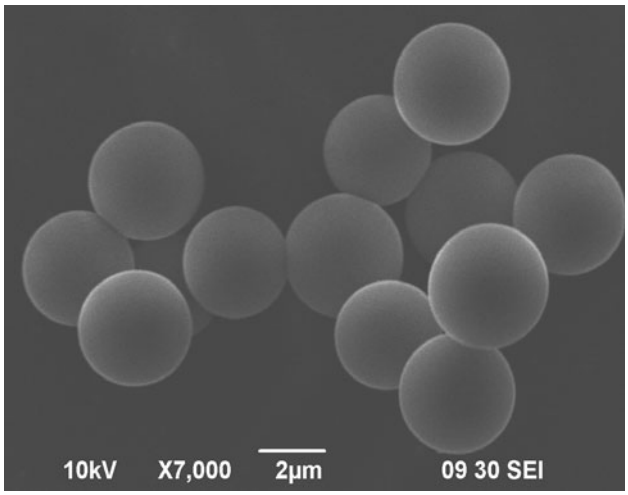

Fig. 4 Carbon spheres

various graphitization stages (Fig. 3). The existence of almost complete drops that remain connected to the cover proves the material's extremely high viscosity, with flow being so slow that the layer graphitized before the drops fell (indicated by arrows in Fig. 3).

Solid spheres are the final product in the container volume, with the appearance of black dust. Their perfect shape (Fig. 4) suggests the following possible mechanism of formation. To be transformed to graphite structure by the pyrolytic process, the starting material has suffered permanent carbon atom restructuring similar to that in the drops on the container cover. While this occurred, the material from which the sphere is formed had sufficient time and space to assemble into a drop under surface tension. Each of the spheres formed as an independent object, which was liquid and subsequently turned into the solid graphitized state, although rarely, broken spheres can be seen, as shown in Fig. 5. None of these is hollow, which proves that the formed spheres are completely solid. Under TEM observation, the spheres do not let rays pass, even when they are of very small size, and they remain black. This is also proof, albeit indirect, of their high density.

From the moment of their formation until final graphitization, the spheres in the container influence one another. When analyzing their contact zones, two cases occur. In the first case, the growth process has finished and the spheres touch without changing their shape or size (Fig. 6). The second case (Fig. 7a), which also occurs often, can only be explained by assuming that the growth process continues after contact of already formed spheres. To improve our understanding of the location of the contact and what happens afterwards, the area framed in Fig. 7a is magnified and shown in Fig. 7b. In the same image, suggested sphere silhouettes at the moment of contact are superimposed as dark circles. Figure 7b shows that the spheres have grown

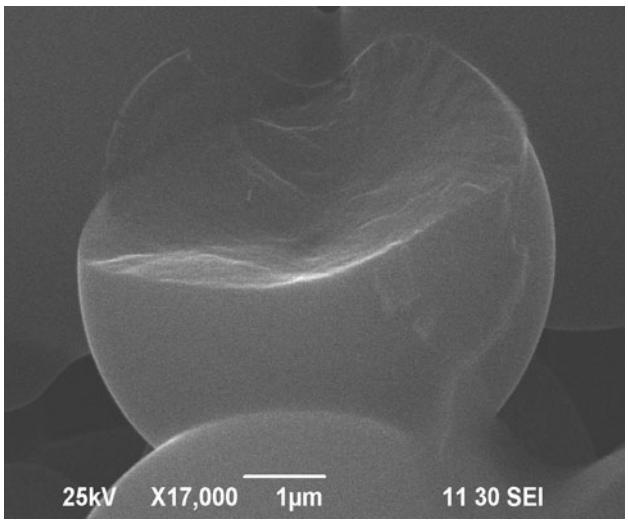

Fig. 5 A broken carbon sphere

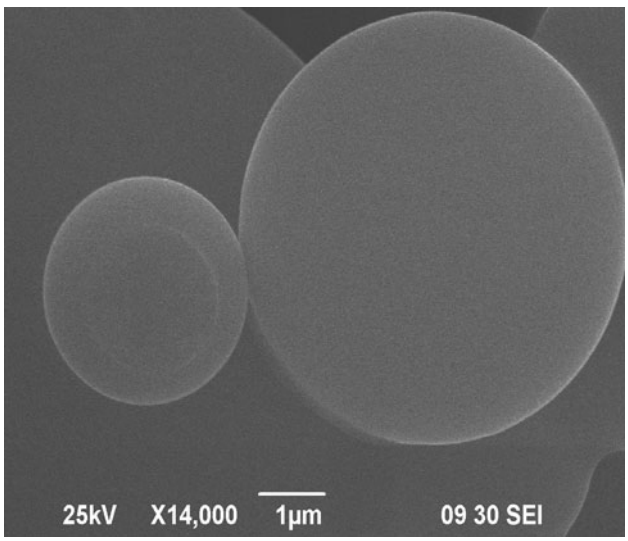

Fig. 6 Touching carbon spheres with no connection between them

exactly concentrically after touching. On the basis of this, we suppose that they were already in the solid state before contacting (otherwise they would amalgamate) and that their growth continued by concentric deposition of still gaseous material supplied by hydrocarbons transforming thereafter. If this is correct, it would be easy to explain the shape of the necks connecting the agglutinated spheres (Fig. 7b). There (zones indicated by arrows), the material is deposited more intensively due to surface forces originating from the small radii of curvature. The neck structure is sometimes incomplete and not mechanically solid. It is often broken, causing the spheres to separate. In Fig. 8, the breakage of a relatively long neck is seen, which shows that sphere connection can occur without their being in contact. An arrow indicates the breakage spot of another sphere in the same figure. Its neck fractured before the snapshot, resulting in the sphere being removed. Such thin neck capture spots are often observed. The location of first contact between the spheres is clearly discernible, and the concentric form of the breakage zone confirms the supposition that neck growth started after contact between already completed spheres, followed by additional concentric growth of the contacting particles. Sometimes this process of sphere contact and fusion can involve a larger number of particles, resulting in the appearance of a pearl necklace (Fig. 9).

If the contact happens when the particles are still liquid, a fusion process starts, driven by the surface energy force to merge the particles and thereby decrease the surface area. Such spheres are indicated by arrows in Fig. 10. The merging process may spread over a large number of particles, resulting in formation of long chains (Fig. 11).

EDS was used to examine the particles' elemental content. The spheres proved to consist of carbon (Fig. 12). Substantial oxygen presence was recorded in the spherical structures, independent of the starting material.

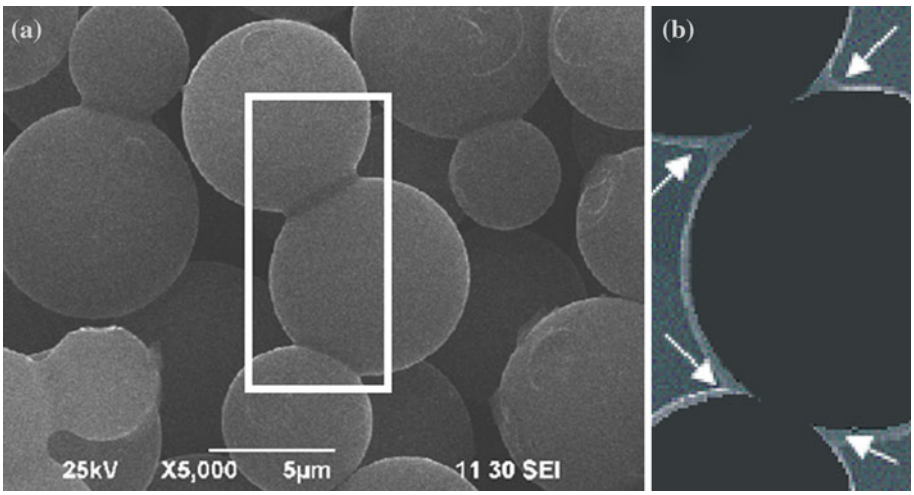

Fig. 7 **a** Connected spheres. The contact zone is outlined in a frame; **b** An enlarged image of the connection zone. *Dark circles* show the state of spheres on contact. The *light halo* is the material added after contact

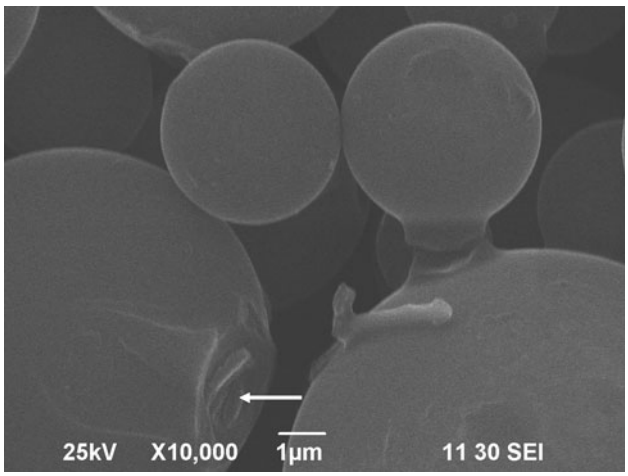

Fig. 8 Connections between remote spheres

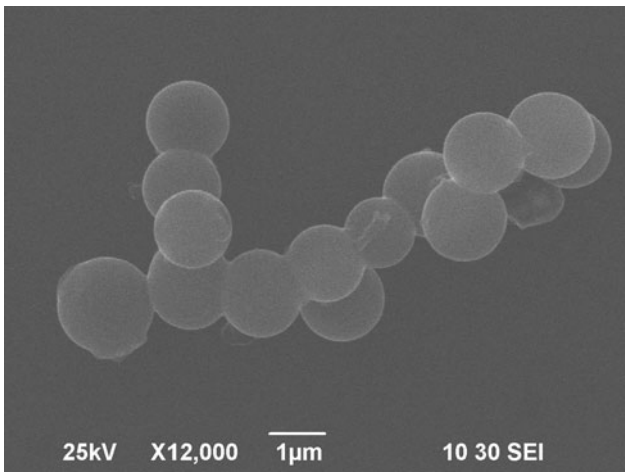

Fig. 9 A pearl necklace of spheres

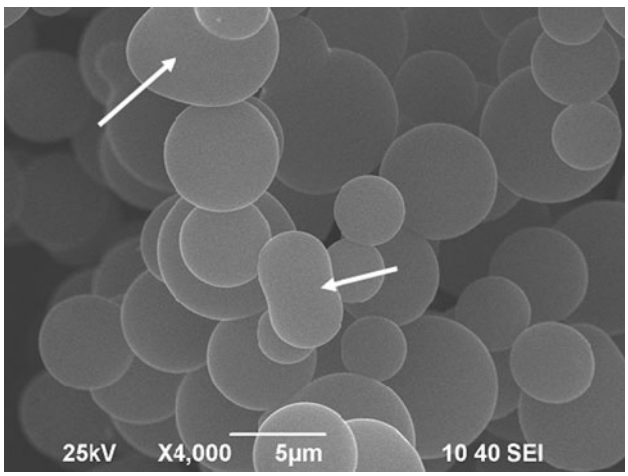

Fig. 10 Coalescence among touching spheres before their solidification

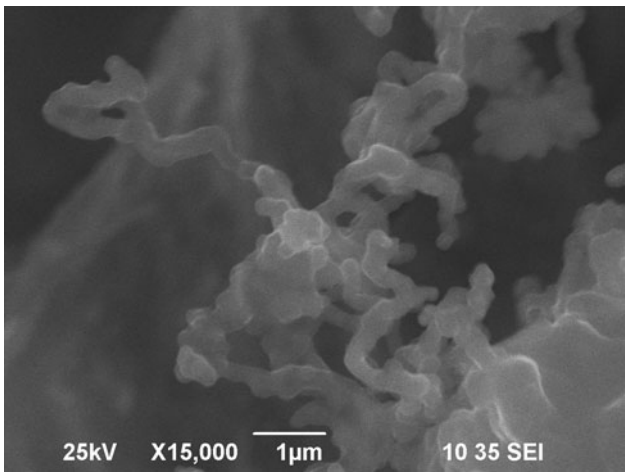

Fig. 11 A chain of agglomerated spheres

The degree of graphitization of the carbon spheres was determined by XRD. Based on the XRD measurements (JCPDS index no. 75-1621), the two observed peaks at 26.2° and 44.3° were found to correspond to (002) and (101) diffraction planes of hexagonal graphitic carbon, respectively. The relatively wide peak at 26.2° indicates that the concentric sphere carbon layers are not completely graphitized and that a certain amount of amorphous carbon is present. Additionally, we assume presence of a lot of graphitized layer edges where atoms from the periphery stand with unsaturated bonds. The number of these bonds can be reduced by provoking additional material graphitization. The easiest way to achieve this is through subsequent high-temperature annealing in an appropriate atmosphere [21]. That was not included in the current experiments, and the measured spheres were not subject to additional graphitization or treated in any other way to improve their structure.

The structure of carbon particles determines their chemical stability. Availability of atoms with free bonds, defects or vacancies in the carbon lattice, and parts filled with amorphous carbon all make such spheres vulnerable to attack by oxygen and hydrogen. The spheres remain stable on heating in inert atmosphere up to 900 °C. They are stable up to about 600 °C in air (Fig. 13). Sphere stability in this temperature interval is expected, since their synthesis has been accomplished at 600 °C in the presence of water vapor as oxidizer.

EDS of air-heated spheres showed oxygen accumulation, which increased for higher sphere treatment temperature. Figure 14 shows the oxygen at.% content after 30 min of treatment at different temperatures. It is clear that temperature stimulates oxygen penetration inside the particles through zones of amorphous carbon and weakly bonded carbon atoms. Above 600 °C, the particle destruction process intensifies. Destruction starts from the

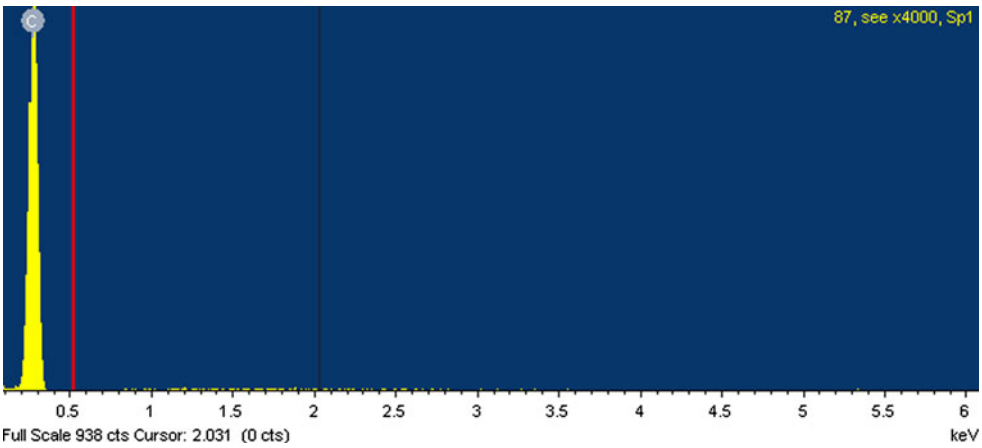

Fig. 12 EDS spectrum of the carbon spheres

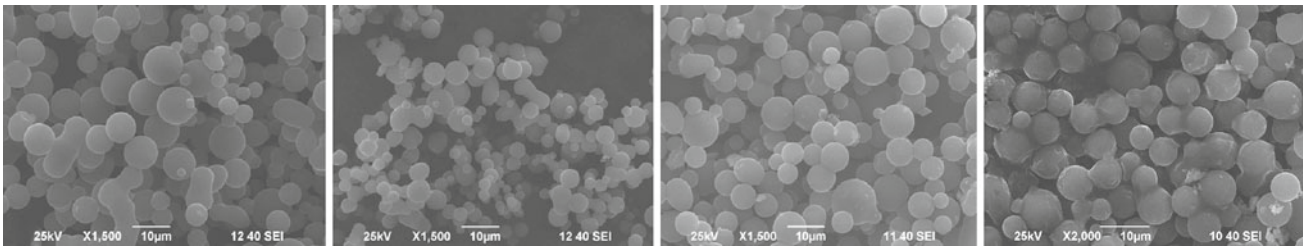

Fig. 13 Spheres treated at 300, 400, 500, and 600 °C for 30 min

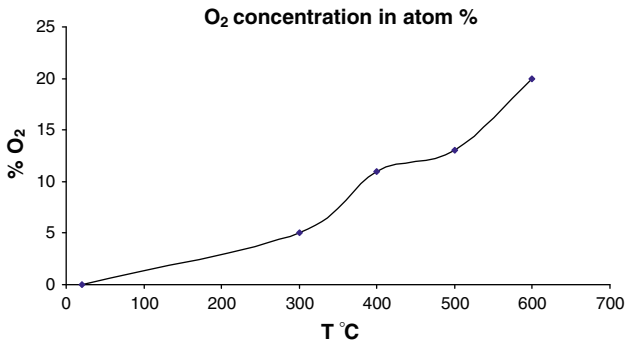

Fig. 14 Oxygen content (in at.%) of spheres treated at different temperatures in air

parts with amorphous carbon and those which are graphitized the least. The process is accelerated by elevated temperature and by increasing oxygen penetration inside the spheres. Figure 15 shows spheres in the process of destruction. As can be seen, only some of the spheres have preserved their shape (indicated with arrows), while for others their previous spherical shape can barely be distinguished. The oxygen content in the partially destroyed structures reaches 20–25 at.%. At temperatures of about 650 °C, full sphere combustion occurs.

In IR spectroscopic measurements (data not shown) of a pressed material tablet of 1 mm thickness, the presence of weak peaks in the absorption curve at 2,880 and 1,720 cm^{-1}

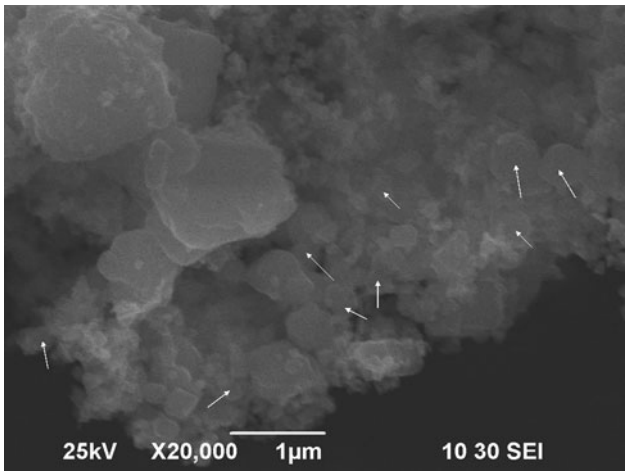

Fig. 15 Spheres destroyed by heating at 650 °C for 30 min. Spheres preserving their shape are indicated by *arrows*

indicates that the spheres contain certain quantities of carbon bonds to hydrogen and oxygen. The availability of vacancies and the presence of other atoms decrease particle stability. On the other hand, this helps to functionalize such structures by incorporating appropriate groups, atoms, and molecules at these locations. This is important if the particles are to be used as fillers, catalysts, for drug delivery, etc.

As mentioned above, the spheres always remain in the container, unlike in other methods described in the literature. Because of this, even minimal variations in local

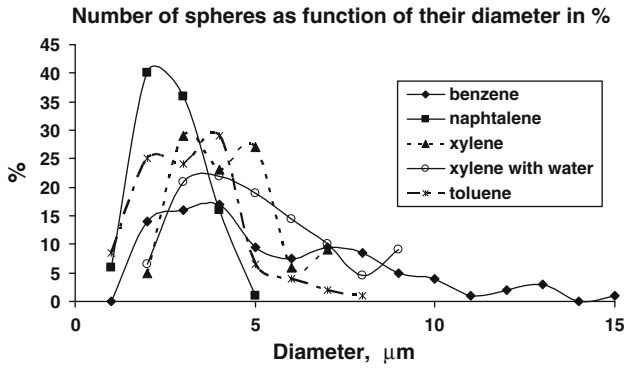

Fig. 16 Diameter distribution of toluene, xylene, benzene, naphthalene, and toluene + water (70/30 vol.%) spheres

conditions may lead to differences in sphere growth and, hence, sphere size. This might be assumed to be a logical explanation for the observed differences in sphere diameter. Sphere diameter is an important parameter for certain application areas, for instance, when used as fillers for composites and electrode materials. Spheres synthesized from different starting materials usually show similar properties but differ in size. Their size distribution is shown in Fig. 16. The observed size difference is related to the chemical nature of the starting materials, which contain different atomic bonds. Hence, precursor decomposition and transformation should proceed under somewhat different conditions, and with differences in the final result.

The edges and planes produced at sphere breakages (Figs. 1, 2, 5) are very even, showing that the atomic bonds are broken along well-defined atomic surfaces. This suggests that the atomic arrangement in the spheres is even, which has not been checked for spheres produced by the two-step pyrolysis method (based on evaporation of the starting material at a given temperature, with subsequent graphitization at high temperature). For example, the spheres reported in [9] clearly exhibit inhomogeneity and internal stratification, and the breakage surfaces are uneven.

Conclusions

The carbon spheres obtained using the described method have relative large diameters due to the peculiarities of the synthesis method. However, they present certain specific characteristics and advantages. The most important advantage is the structural homogeneity of the spheres, which is a reason to expect greater chemical stability and better mechanical properties. The similar results obtained after pyrolytic synthesis based on different cyclic hydrocarbons indicate that the chemical composition of the starting material does not play a substantial role in the sphere synthesis. The only observed difference was in the size of the spheres produced, which is related to the fact that the pyrolytic process starts with a different substance and proceeds with certain variations in the successive transformations until the final sphere graphitization.

Analysis of the synthesized products of cyclic hydrocarbon pyrolysis allows the route of formation and growth of spherical structures to be determined as occurring in the vapor–liquid–solid state and without a substrate as process moderator.

Sphere stability is decreased by the presence of amorphous carbon and defects in the partially graphitized layers of the spheres. When spheres are treated in air, oxygen attack becomes substantial. The amount of hydroxyl groups increases with temperature, and above 600 °C, intensive material decomposition starts. This is due to increased oxygen penetration via structural defects and due to activation of the chemical reaction itself. The presence of defects in the spheres yields the possibility of influencing their chemical activity. Through appropriate functionalization, spheres can be applied for catalyst applications and in a wide range of chemical and biological systems. The low weight of these carbon structures and their attractive chemical and physical properties enable their possible use as components in light, chemically stable composite materials for various applications, even for aerospace applications.

Acknowledgement This work was supported by the Bulgarian Science Foundation (contract no. DOO2-241/18.12.2008), which is gratefully acknowledged.

References

1. Iijima S (1980) J Cryst Growth 50:675
2. Kroto HW, Heath JR, O'Brien SC, Curl RF, Smalley RE (1985) Nature 318:162
3. Iijima S (1991) Nature 354:56
4. Wang YG, Korai Y, Mocbida I (1999) Carbon 37:1049
5. Xu CW, Cheng LQ, Shen PK, Liu YL (2007) Electrochem Commun 9:997
6. Liu YC, Qiu XP, Huang YQ, Zhu WT (2002) Carbon 40:2375
7. Alcántara R, Fernández Madrigal FJ, Lavela P, Tirado JL, Jiménez Mateos JM, Gómez de Salazar C, Stoyanova R, Zhecheva E (2000) Carbon 38:1031
8. Chen J, Xia N, Zhou T, Tan S, Jiang F, Yuan D (2009) Int J Sci 4:1063
9. Jin YZ, Gao C, Hsu WK, Zhu Y, Huczko A, Bystrzejewski M, Roe M, ChY Lee, Acquah S, Kroto H, Walton DRM (2005) Carbon 43:1944
10. Zhao Sh, Wang Ch, Chen M, Shi Zh (2008) Mater Lett 62:3322
11. Pradhan D, Sharon M (2002) Mater Sci Eng B96:24
12. Yan XB, Xu T, Xu S, Chen G, Liu HW, Yang SR (2004) Carbon 42:2735
13. Xu S, Yan XB, Wang XL, Yang SR, Xue QJ (2010) J Mater Sci 45:2619. doi:10.1007/s10853-010-4239-4
14. Nieto-Marquez A, Espartero I, Lazo JC, Romero A, Valverde JL (2009) Chem Eng J 153:211
15. Liu B, Jia D, Rao J, Meng QC, Shao Y (2008) Bull Mater Sci 31(5):771

16. Miao J-Y, Hwang DW, Narasimhulu KV, Lin P-I, Chen Y-T, Lin S-H, Hwang L-P (2004) Carbon 42:813
17. Koprinarov N, Marinov M, Pchelarov G, Konstantinova M, Stefanov R (1995) J Phys Chem 99:2042
18. Koprinarov N, Konstantinova M, Ruskov T, Spirov I, Marinov M, Tsacheva Ts (2007) Bulg J Phys 34:17
19. Croweley C, Taylor R, Kroto H, Walton D, Cheng P-Ch, Scott L (1996) Synth Met 77:17–22
20. Orlanducci S, Valentini F, Piccirillo S, Terranova ML, Botti S, Ciardi R, Rossi M, Palleschi G (2004) Mater Chem Phys 87:190
21. Kasahara N, Shiraishi S, Oya A (2002) Carbon 411:1645